

Ab initio study of the transition states for determining the enthalpies of formation of alkyl and halogenated alkyl free radicals†

Jorma A. Seetula

Laboratory of Physical Chemistry, P.O. Box 55 (A.I. Virtasen aukio 1), FIN-00014, University of Helsinki, Helsinki, Finland. E-mail: Jorma.Seetula@csc.fi

Received 18th February 2000, Accepted 11th July 2000

Published on the Web 16th August 2000

Enthalpies of formation of 19 free radicals at 298 K are calculated by *ab initio* methods. The equilibrium reactions of radical + HBr \rightleftharpoons molecule + Br were studied by optimizing the transition states of the reactions at the MP2(fc)/6-31G(d,p) level of theory. The *ab initio* calculated threshold energies of the reverse reactions were combined with the experimentally determined activation energies of the forward reactions in a second-law method to determine the enthalpies of the reactions. The enthalpy of formation values are (in kJ mol⁻¹): 149.3 \pm 2.8 (CH₃), 172.5 \pm 3.7 (CH₂Br), 121.7 \pm 4.5 (CH₂Cl), 180 \pm 5 (CHBr₂), 145 \pm 8 (CHBrCl), 92.2 \pm 3.9 (CHCl₂), 195 \pm 5 (CBr₃), 163 \pm 8 (CBr₂Cl), 124 \pm 8 (CBrCl₂), 70.6 \pm 3.7 (CCl₃), 120.4 \pm 2.7 (CH₃CH₂), 81.1 \pm 2.9 (CH₃CHCl), 99.7 \pm 2.9 (CH₂ClCH₂), 46.0 \pm 3.2 (CH₃CCl₂), 90.1 \pm 3.2 (CHCl₂CH₂), 102.5 \pm 2.8 (*n*-C₃H₇), 83.6 \pm 2.8 (iso-C₃H₇), 29.9 \pm 3.0 (2-iso-C₃H₆Cl), 80.7 \pm 2.8 (*n*-C₄H₉). The chemical nature of the transition states was studied by localizing them along the minimum energy path of the reaction.

Introduction

The heat of formation values of free radicals are useful for determining bond enthalpies of molecules and kinetic parameters of the reactions where these species are involved. Especially, bond enthalpies are fundamental for chemistry: thermochemical and kinetic information about compounds and their reactions are much needed; for example, to model various chemical processes.

Typically, heat of formation values of free radicals have been determined by kinetic methods in which both reaction directions of the equilibrium reaction are measured in a gas phase as a function of temperature. This kinetic information is used with second-law and third-law methods to determine the thermodynamic parameters for free radicals.¹ However, such studies are typically restricted to the most stable free radical isomers and light molecular species. Of bromine-containing species only the CH₂Br radical has been a subject of time-resolved kinetic investigations.² Obviously, the CH₂Br radical can be formed from methyl bromide by a hydrogen atom abstraction reaction. Accurate thermochemical information about this radical is important since methyl bromide is widely used as a pesticide. Moreover, polybrominated free radical reactions are not measured by time-resolved techniques. Some thermodynamic parameters of these species have been obtained by conventional techniques.^{3,4}

The current study presents an *ab initio* investigation of the threshold energies of Br atom reactions with alkanes and halogenated alkanes. These calculated energies are combined with the experimentally determined activation energies of the forward reactions to determine the enthalpies of formation of the free radicals studied. Another function of the current study was to investigate the effects of halogen and alkyl substituents on the transition state of the radical + HBr \rightleftharpoons molecule + Br equilibrium. Alkylation and halogenation have been experimentally proved to have a strong effect on the kinetics of

various free radical reactions with molecules such as HI and HBr.^{1,5}

Free radical reactions

The thermodynamics of the following 19 free radical equilibrium reactions with HBr have been studied using quantum chemical calculations:



Here R = CH₃, CH₂Br, CH₂Cl, CHBr₂, CHBrCl, CHCl₂, CBr₃, CBr₂Cl, CBrCl₂, CCl₃, CH₃CH₂, CH₃CHCl, CH₂ClCH₂, CH₃CCl₂, CHCl₂CH₂, *n*-C₃H₇, iso-C₃H₇, 2-iso-C₃H₆Cl or *n*-C₄H₉. The optimized saddle points were characterized by only one negative value of the second derivative of the potential energy surface. The temperature of the reactions for the *ab initio* calculations is taken to be absolute zero.

Computational details

Ab initio calculations were carried out with the GAUSSIAN 94 package of programs.⁶ All calculations were carried out on an SGI Power Challenge computer at the Centre for Scientific Computing (Espoo, Finland). All structures of species needed for transition state calculations were fully optimized at the MP2 level of theory using the 6-31G(d,p) basis set and frozen-core approximation.⁷ These Born–Oppenheimer structures were shown to be at their local minimums by analytical gradient methods. In a zeroth-order approximation the reaction takes place along the lowest-energy path connecting the reactants and the products of the reaction (tunneling is ignored). The transition state of the reaction⁸ was localized at this path using a quadratic synchronous transit method.⁷ In the calculations the expectation values, S^2 , for free radicals were in the range 0.7561–0.7722 and for transition states from 0.7698 to 0.7907. Normal mode analyses were carried out at the same level of theory for all species and transition states. These frequency calculations show the optimized transition states to be

† Electronic Supplementary Information available. See <http://www.rsc.org/suppdata/cp/b0/b001350/>

first-order saddle points with all the second derivatives of energy being positive except for one, which has an imaginary vibrational frequency (*i.e.* the force constant matrix has only one negative eigenvalue) along the reaction coordinate. In this case, the polyatomic potential energy surface is a minimum in other dimensions, while along the reaction coordinate it is a maximum.⁷ The imaginary frequencies were in the range of -164 to -1250 cm^{-1} . The internal coordinates of the transition states, which according to the calculated normal modes experience the largest changes during the reaction, are the C–H and H–Br bond lengths. The relative movement of the H atom is the largest. The C–H–Br asymmetric stretch is the reaction coordinate. Furthermore, zero-point energies of species were multiplied by 0.9676 for the energy calculations.⁷ The zero-point energy corrected energies of the reactants and the products were compared to those of the reaction transition states (Table 1). Geometries and frequencies of the transition states, molecules and free radicals involved in the current study are given as supplementary material.†

Activation energies of Br + RH reactions, reverse reaction

Generally the MP2/6-31G(d,p) level of theory is not adequate for accurate transition state energy calculations, but obviously at this level there exists a successful error cancellation in determining the activation energies of the reactions of Br atom with closed shell hydrocarbons. These MP2 calculations turned out to be surprisingly accurate.

Scaled zero-point energy-corrected MP2 energies of the transition state and the products of the forward reaction were used for the calculations. The calculated threshold energies of the reverse reactions turned out to deviate from -4.3 to 4.4 kJ mol^{-1} compared to the experimentally determined activation energies (see Table 2). However, such deviations are relatively small if typical error limits of ± 2.5 kJ mol^{-1} for the experimentally determined activation energies are considered. For bimolecular reactions the calculated threshold energy E_0 is related to the Arrhenius activation energy, according to line-of-centers collision theory,⁹ by a simple equation: $E_a = E_0 + \frac{1}{2}RT$. At the absolute zero, E_a equals E_0 exactly. A canonical transition state theory would likely correct the calculated E_0 values by $\pm \frac{1}{2}RT$ if the temperature dependency of a vibrational partition function is considered to vary from T^0 to $T^{1/2}$.

Activation energies of R + HBr reactions, forward reaction

The reactions of free radicals with HBr are strongly exothermic processes, by a similar amount of enthalpy. Thus, the reaction enthalpy change is less meaningful for determining the order of radical reactivity.² On the other hand, the kinetics are related to reactivity. Moreover, the kinetics of the forward reactions can be successfully explained by plotting the rate constant of the reactions at one temperature *vs.* the change in electronegativity values of the radicals.² The change in electronegativity is the difference between the sum of electronegativities of the three atoms or groups in the substituted methyl radical and the sum of electronegativities of the three hydrogen atoms in an unsubstituted methyl radical.² The values of electronegativities for atoms (Pauling's electronegativities) are Cl (3.16), Br (2.96), H (2.20) and for 1.82 CH_3 .² This method can also be used to estimate the kinetics of an unknown radical reaction. The reactivity trend in the plot is caused, principally, by the activation energies of the reactions because of their exponential effect on the rate constants. Thus a plot of various activation energies of the

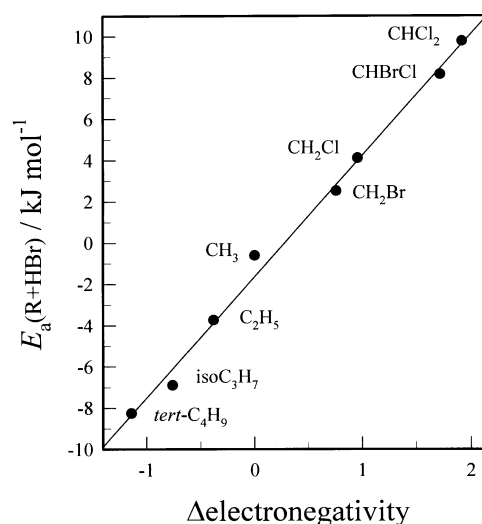


Fig. 1 Plot of the experimentally determined activation energies of R + HBr reactions as a function of electronegativity difference. Electronegativities of elements are taken from Pauling.³⁰ The fitted linear function is $y = -1.62 + 5.88x$.

Table 1 Structural parameters and energies of the calculated $\text{R}\cdots\text{H}\cdots\text{Br}$ transition states and of the HBr molecule for comparison. Bond lengths and r^\ddagger are given in pm, angles in degrees and energies in E_h . Calculations were done at the MP2(fc)/6-31G(d,p)/MP2(fc)/6-31G(d,p) level of theory. The $\Delta r_{\text{C-H}}$ values are given in percentages and $r^\ddagger = [r_{\text{Br-H}}(\text{TS}) - r_{\text{Br-H}}(\text{HBr})] - [r_{\text{C-H}}(\text{TS}) - r_{\text{C-H}}(\text{RH})]$. Structural parameters and energies for the other species involved are given as supplementary material

R	r^\ddagger	$r_{\text{C-H}}$	$\Delta r_{\text{C-H}}$	$r_{\text{H-Br}}$	$a_{\text{C-H-Br}}$	Zero-point-energy	MP2 energy
CH_3	-39.9	158.2	45.7	150.3	0.0	0.038 926	-2610.285 178
CH_2Br	-34.7	153.7	41.9	151.3	6.9	0.030 888	-5179.693 207
CH_2Cl	-31.4	151.5	39.7	152.3	3.9	0.031 508	-3069.303 946
CHBr_2	-28.6	148.7	37.4	152.5	-5.5	0.021 411	-7749.102 028
CHBrCl	-26.1	147.1	35.8	153.3	-4.6	0.022 182	-5638.711 637
CHCl_2	-23.7	145.6	34.4	154.2	-3.4	0.022 948	-3528.321 741
CBr_3	-21.7	143.4	32.5	154.1	0.0	0.010 959	-10 318.510 520
CBr_2Cl	-20.1	142.6	31.7	154.8	-1.3	0.011 854	-8208.118 587
CBrCl_2	-19.0	141.9	31.1	155.3	1.4	0.012 664	-6097.726 937
CCl_3	-17.5	141.1	30.3	155.9	0.0	0.013 450	-3987.335 633
CH_3CH_2	-42.6	160.7	47.6	149.8	-6.4	0.069 842	-2649.472 674
CH_3CHCl	-32.3	152.4	40.2	152.0	-7.2	0.061 405	-3108.497 098
CH_2ClCH_2	-40.9	159.0	46.2	149.9	-8.0	0.061 275	-3108.489 619
CH_3CCl_2	-23.9	145.9	34.4	154.0	-7.5	0.052 167	-3567.518 089
CHCl_2CH_2	-40.1	158.1	45.3	149.8	-7.3	0.051 489	-3567.503 417
$\text{CH}_3\text{CH}_2\text{CH}_2$	-44.9	162.6	49.2	149.3	-7.0	0.099 677	-2688.654 415
$(\text{CH}_3)_2\text{CH}$	-50.6	167.3	53.2	148.1	-8.1	0.099 773	-2688.662 112
$(\text{CH}_3)_2\text{CCl}$	-36.2	155.5	42.8	151.0	-9.2	0.090 838	-3147.690 794
$\text{CH}_3\text{CH}_2\text{CH}_2\text{CH}_2$	-44.9	162.6	49.2	149.3	-6.5	0.129 073	-2727.836 842
HBr	—	—	—	140.6	—	0.006 300	-2570.592 802

Table 2 Activation energies of the $R + HBr \rightleftharpoons RH + Br$ equilibrium; calculated activation energies are at absolute zero and measured activation energies at the mean temperatures of the used temperature ranges for experimental studies

R/RH	$E_a(R + HBr)^a/kJ mol^{-1}$	$E_a(Br + RH)/kJ mol^{-1}$ calculated	$E_a(Br + RH)^a/kJ mol^{-1}$ measured
CH ₃	-0.6		
CH ₄		73.3	76.1 ± 3.7
CH ₂ Br	2.5		
CH ₃ Br		63.1	64.4 ± 2.4
CH ₂ Cl	4.1		
CH ₃ Cl		59.3	57.7 ± 2.3
CHBr ₂	7.4 ^b		
CH ₂ Br ₂		49.0	n.a. ⁱ
CHBrCl	8.2		
CH ₂ BrCl		48.4	n.a.
CHCl ₂	9.8		
CH ₂ Cl ₂		47.9	47.0 ± 2.5
CBr ₃	11.9 ^b		
CHBr ₃		34.1	n.a.
CBr ₂ Cl	13.0 ^b		
CHBr ₂ Cl		35.6	n.a.
CBrCl ₂	14.2 ^b		
CHBrCl ₂		37.5	n.a.
CCl ₃	15.4 ^b		
CHCl ₃		39.8	38.9 ± 2.5 ^h
CH ₃ CH ₂	-3.7		
CH ₃ CH ₃		50.4	53.3 ± 2.1
CH ₃ CHCl	-3.0		
CH ₃ CH ₂ Cl		40.3 ^c	37.8 ± 1.5 ^c
CH ₂ ClCH ₂	-2.2		
CH ₃ CH ₂ Cl		59.6 ^d	55.3 ± 2.3 ^d
CH ₃ CCl ₂	5.9		
CH ₃ CHCl ₂		32.5 ^c	30.9 ± 1.4 ^c
CHCl ₂ CH ₂	-0.7 ^e		
CH ₃ CHCl ₂		69.3 ^d	n.a.
iso-C ₃ H ₇	-6.9		
C ₃ H ₈		31.6 ^f	36.0 ± 2.0 ^f
n-C ₃ H ₇	-5.4		
C ₃ H ₈		51.5 ^g	53.3 ± 2.1 ^g
2-iso-C ₃ H ₆ Cl	-0.4 ^b		
2-C ₃ H ₇ Cl		24.8 ^f	n.a.
n-C ₄ H ₉	-6.4		
n-C ₄ H ₁₀		50.6 ^g	53.3 ± 2.1 ^g

^a See references for the experimentally measured E_a values in Table 4. ^b Value obtained from the linear regression equation. ^c α -Hydrogen abstracted. ^d β -Hydrogen abstracted. ^e Estimated by comparing measured E_a values of the CH₃CH₃ and the CH₂ClCH₂ radicals with HBr. ^f Secondary hydrogen abstracted. ^g Primary hydrogen abstracted. ^h See ref. 31. ⁱ Not available.

radical + HBr reactions against the change in electronegativity values of the radicals involved should indicate a linear dependency, which is shown in Fig. 1. This linear relationship is used to determine the activation energies of those R + HBr reactions which have not been determined experimentally (see Table 2).

Table 3 Heats of formation used in the thermochemical calculations

Species	$\Delta_f H_{298}^\circ/kJ mol^{-1}$	Ref.
HBr	-36.44 ± 0.17	10
Br	111.86 ± 0.06	10
CH ₄	-74.87 ± 0.34	10
CH ₃ Br	-38.1 ± 1.3	11
CH ₃ Cl	-83.68 ± 2.1	10
CH ₂ Br ₂	-11.1 ± 5.0	11
CH ₂ BrCl	-44.8 ± 8.2	12
CH ₂ Cl ₂	-95.52 ± 1.3	10
CHBr ₃	23.8 ± 4.5	11
CHBr ₂ Cl	-8.9 ± 8.2	12
CHBrCl ₂	-48.8 ± 8.2	12
CHCl ₃	-103.18 ± 1.3	10
CH ₃ CH ₃	-83.9 ± 0.3	13
CH ₃ CH ₂ Cl	-112.1 ± 0.5	14
CH ₃ CHCl ₂	-130.1 ± 0.8	15
C ₃ H ₈	-104.5 ± 0.3	14
2-C ₃ H ₇ Cl	-145.0 ± 0.6	14
n-C ₄ H ₁₀	-126.5 ± 0.4	14

Thermochemical calculations

In the reactions of the $R + HBr \rightleftharpoons RH + Br$ equilibrium no mole change is involved. Consequently, the standard reaction enthalpy change, $\Delta_r H^\circ$, is simply the difference between the activation energies of the reactions in each direction. The mean temperature on a $1/T$ scale of the studied reaction directions is always near 0 K if the other activation energy is determined at absolute zero. Thus the $\Delta_r H^\circ$ value obtained should be corrected to 298 K using a heat capacity correction according to Kirchhoff's equation. For these calculations the heat capacity values at constant pressure of Br and HBr were taken from the literature. For the other compounds studied, the *ab initio* calculated heat capacity values at constant volume were used instead. However, for an ideal gas reaction with no mole change these two heat capacities are similar ($\Delta C_p^\circ = \Delta C_v^\circ + \Delta nR$). In addition, the heat capacities of all compounds equal 0 at absolute zero. If a polynomial expression, $a + bT + cT^2$, for a heat capacity is used then the mean standard heat capacity of the reaction is obtained simply by eqn. (2).

$$\Delta \bar{C}_p^\circ(\Delta T) = \frac{1}{2}[\Delta C_p^\circ(T_1) + \Delta C_p^\circ(T_2)] - \frac{c}{6} \Delta T^2$$

$$\approx \frac{1}{2} \Delta C_p^\circ(298) \quad (2)$$

The standard enthalpy of formation values of free radicals, $\Delta_f H_{298}^\circ$, were ultimately calculated using $\Delta_r H_{298}^\circ$ and the

tabulated heat of formation values of Br, HBr and molecules (see Table 3). Typically for reactions which involve species containing many bromine atoms, the heat of formation value has a low accuracy. The reason for this lies in the substantial uncertainty of the heat of formation values of the brominated molecules (see Table 3).

Discussion

Structures of transition states

Some parameters of the optimized transition state structures are shown in Table 1. The transition state is the same in the both reaction directions. The location of the transition state is discussed in detail in a separate section. Two critical bond lengths and one bond angle of the transition states are given. For the reverse Br + alkane reactions the forming H–Br bond length ($r_{\text{H-Br}}$) is shorter than the breaking C–H bond length ($r_{\text{C-H}}$). However, for Br + halogenated alkane reactions, the forming H–Br bond length is typically the longer of these two bonds. The breaking C–H bond length increases as a function of alkylation and decreases as a function of halogenation. By way of comparison, halogenation and alkylation have similar effects, as shown in the current study, at the transition states of the equilibrium reactions of $\text{R}' + \text{Cl}_2 \rightleftharpoons \text{R}'\text{Cl} + \text{Cl}$ ($\text{R}' = \text{CH}_3, \text{CH}_2\text{Br}, \text{CH}_2\text{Cl}, \text{CHBrCl}, \text{CHCl}_2, \text{CCl}_3, \text{CH}_3\text{CH}_2$ or CH_3CCl_2).¹⁶

As expected, the transition states for $\text{CH}_3, \text{CBr}_3$ and CCl_3 radicals are symmetrical tops (see Table 1). For the other transition states studied, the interacting out-of-line angle of the centers of the reactants ($a_{\text{C-H-Br}}$) varies between -9.2 and 6.9° . The H–Br bond of these transition states is bent away from the large substituent(s) of the radical. A similar trend of the interacting out-of-line angles of the reactants at the transition states of the $\text{R}' + \text{Cl}_2$ reactions exists.¹⁶

Br + RH reactions

Because a bromine atom abstraction reaction on a saturated hydrocarbon is a strongly endothermic process, the thermochemistry of the reaction determines to a large extent the kinetics of the reaction. The size of the energy barrier reflects the bond strength of the breaking C–H bond of the alkane. Both alkylation and chlorination lower the energy barrier of the abstraction reaction. For example, by comparing the activation energies of the reverse reactions in Table 2, it can be seen that the reaction of $\text{Br} + \text{C}_3\text{H}_8 \rightarrow \text{iso-C}_3\text{H}_7 + \text{HBr}$ has an activation energy that is 19.9 kJ mol^{-1} smaller than that of the reaction of $\text{Br} + \text{C}_3\text{H}_8 \rightarrow n\text{-C}_3\text{H}_7 + \text{HBr}$. This harmonizes with the C–H bond strengths of propane: the secondary bond is 14 kJ mol^{-1} weaker than the primary bond.⁵

R + HBr reaction

The forward reaction between a free radical and hydrogen bromide is a strongly exothermic process, and for σ -radical reactions by a similar amount. The thermochemistry of the reaction has a smaller effect on the reaction kinetics of exothermic reactions than that of endothermic reactions. Other phenomena, such as electrostatic effects, exercise strong control over the kinetics of exothermic reactions. These effects appear as unexpected temperature dependencies of free radical + HBr reactions. For alkyl radical + HBr reactions, negative temperature dependencies have been observed experimentally.^{5,17} The activation energies of these reactions are explained generally by a complex reaction mechanism that involves two transition states. The first, with no threshold energy, is a loose transition state (a bound complex), which has a high density of states, and the second is a tight transition state (an activated complex).¹⁸ All optimized transition states in the current study are considered to be the latter type.

In this kind of metathesis reaction the radical may initially be attracted loosely to the Br end of HBr. Such a complex is postulated to have a bent structure.¹⁹ The reaction proceeds by rotating the Br–H, thereby forming an almost collinear tight $\text{R}\cdots\text{H}\cdots\text{Br}$ transition state, which leads to the products of the reaction. The rotation becomes energetically increasingly more feasible if the distance between C and Br increases while the H end of HBr rotates toward the carbon atom. For instance, for the reaction $\text{CH}_2\text{Br} + \text{HBr} \rightleftharpoons \text{CH}_3\text{Br} + \text{Br}$, both a bent transition state and a linear transition state, in which the radical is bonded to the Br end of HBr, were located at the MP2(fc)/6-31G(d,p) level of theory. Fig. 2 demonstrates energies of the transition states, reactants and products of this reaction. As shown in the insert of Fig. 2, a rotation barrier exists between the bent and the linear transition states. The barrier still exists even if the distance between C and Br is extended to be similar to that in the $\text{CH}_2\text{Br}\cdots\text{H}\cdots\text{Br}$ transition state. As shown, the threshold energy for forming the bent transition state is high. If the CH_2Br is initially attracted to the Br end of HBr in the formation of the bent transition state, this may cause the rotation of the BrH or the migration of the CH_2Br towards the H end of BrH to occur. If this is the case, the reaction could be described as a microscopic branching reaction which facilitates the formation of internally differently excited CH_3Br .²⁰ Otherwise, the linear transition state proceeds to the formation of $\text{CH}_2\text{Br}_2 + \text{H}$ as products of the reaction *via* macroscopic branching.

The measured negative temperature dependencies of $\text{R} + \text{HBr} \rightarrow \text{RH} + \text{Br}$ reactions^{5,17} imply that the activated complex formed at the second transition state has increasing possibility as a function of alkylation of the complex to decompose back to the reactants of the reaction as the temperature of the reaction increases.⁵ The activated complex should be thermally excited more easily if a high density of states is available. To study the decomposition processes of transition states, the number of vibrational states as a function of energy at the transition state were qualitatively calculated

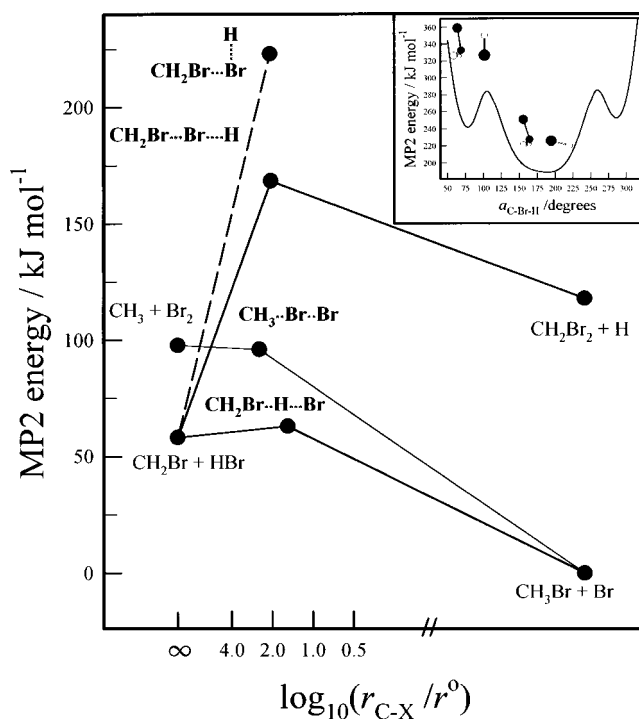


Fig. 2 Profile of the potential energy surface of the $\text{CH}_2\text{Br} + \text{HBr}$ reaction at the MP2(fc)/6-31G(d,p) level of theory. The logarithm of the approaching coordinate $r_{\text{C-X}}$ ($\text{X} = \text{H}$ or Br) is used to place the barrier crests along the reaction paths. For clarity, the products are moved to the right of their original places. The insert shows the potential energy of the transition state after rotating H of HBr in the plane of the figure.

using the Marcus–Rice expression and the *ab initio* calculated transition state frequencies with zero-point energy corrections.²¹ The results demonstrate that the number of states as a function of energy is larger for the transition states of iso-C₃H₇ + HBr and CH₂ClCH₂ + HBr reactions than for *n*-C₃H₇ + HBr and CH₃CHCl + HBr reactions, for example.

Nature of the transition state

The size of the energy barrier is controlled by electrostatic effects. Obviously the same phenomena control the location of the transition state along the reaction coordinate. This can be studied, for instance, by comparing the forward reactions.

All the previously studied exothermic radical + Cl₂ reactions using the *ab initio* method have an early transition state, thus being reactant in nature.^{16,22} On the other hand, the radical + HBr reactions can be considered to have an earlier transition state for alkyl radical reactions and a later transition state for halogenated alkyl radical reactions. Generally, as the radical + HBr reactions studied are all exothermic processes, the transition state is placed on the entrance channel of the reaction potential energy surface. However, the transition state (the barrier crest) does not systematically move to earlier positions as the exothermicity of the R + HBr reaction increases. Instead an increasingly early energy release (*i.e.* attractive energy release) of the reaction exothermicity in the entrance channel of the forward reaction is reflected in a higher internal excitation in the products of the reaction.²³

The H atom abstraction reactions studied can be considered to be interactions of a heavy object (R for forward reaction and Br for reverse reaction) with a light–heavy mass combination, R··H··Br, where the light object H is removed in recoil of it. This causes the R–H compound being formed to be vibrationally excited.²³ Elongation of the forming C–H bond of the forward reaction compared to its equilibrium bond length in the stable molecule differs greatly for various reactions. As shown in Table 1 as Δr_{C-H} values, the change is the largest for the iso-C₃H₇ + HBr reaction and the smallest for the CCl₃ + HBr reaction. This indicates that the products of the iso-C₃H₇ + HBr reaction are more vibrationally excited than those of the CCl₃ + HBr reaction. On the other hand the products of the reverse reactions are only modestly vibrationally excited, as a small change in the breaking bond length of HBr shows in Table 1. Furthermore, the transition states studied are typically bent, which implies that the products are also rotationally excited.

Location of the transition state

The attractive energy release is expressed as a relative location of the transition state at the reaction coordinate in Fig. 3. As a matter of fact, the reaction barrier should be described in a mass-weighted coordinate system. However, when the reactions studied here are considered to be interactions of the mass combination mentioned above, the scaling factor is similar and the skewed angle between the coordinates has a value between 16 and 7°. The exit channel is bent over the entrance channel in a similar manner for all the reactions studied. Thus it suffices that only the exit channels of the Br atom reactions (which are the entrance channels of the forward reactions discussed above) are presented in Fig. 3. This figure is a three-dimensional (3D) plot where the *z*-axis = the *ab initio* calculated activation energies of Br + molecule → HBr + α -radical reaction, the *x*-axis = the difference in electronegativity values² normalized to that of CH₄, and the *y*-axis = the barrier location expressed as $[r_{Br-H}(TS) - r_{Br-H}(HBr)] - [r_{C-H}(TS) - r_{C-H}(RH)]$.²³ In this equation the extensions of the forming and the breaking bonds of the transition state are compared to the normal equilibrium bond lengths of the free HBr and RH molecules. This

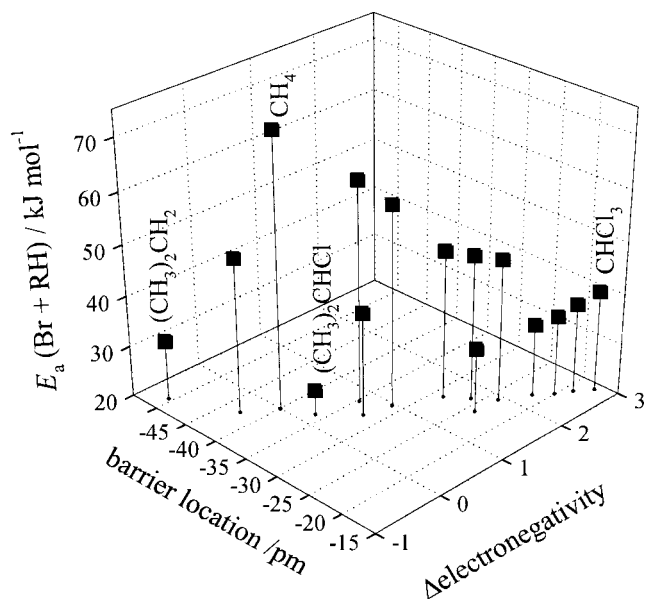


Fig. 3 The barrier location of Br + RH reaction as a function of electronegativity difference values of RH (normalized to CH₄) and the *ab initio* calculated barrier sizes in a 3D plot. The negative barrier location values indicate the distance in pm from a point where the barrier of a thermoneutral reaction such as Br + HBr ⇌ HBr + Br is placed after viewing along the entrance channel of the Br + RH → HBr + R reaction.

procedure yields negative values for endothermic reactions (*i.e.* reverse reactions) because the transition states of such reactions are considered to be late and are placed on the exit channels. Experimental evidence for this is provided in a crossed-molecular-beam experiment of the reaction Br + CH₃I. The product IBr was concluded to be formed by a rebound mechanism,²⁴ which indicates that the transition state is on the exit channel of the endothermic reaction direction.

In a thermoneutral reaction the barrier location equals 0 pm in Fig. 3. The *x*–*y*-plane of the 3D plot expresses the linear behaviour of the barrier locations as a function of the change in electronegativity values (see small solid dots on the plane). This indicates that the location of the transition state is strongly controlled by the electrostatic interactions of the reactants. The lengths of the vertical solid lines demonstrate the heights of the barriers for endothermic reactions. In comparing the activation energies of Br atom reaction with propane, methane and chloroform, one notes that the barrier location is only roughly (*i.e.* late or early location) controlled by the thermochemistry of the reaction. In addition, the barrier sizes are strongly controlled by intramolecular effects. This can be seen in the case of (CH₃)₂CHCl. Attractive energy release for exothermic reaction direction increases as the barrier location value on Fig. 3 becomes more negative. Moreover, attractive energy release is inversely related to the free energy of activation of the reaction, which, on the other hand, is related to kinetics of the reaction.¹⁶

The largest attractive energy release and the loosest transition state come with α -alkylation. Thus, the iso-C₃H₇ + HBr reaction has the loosest transition state of the studied reactions. The high reactivity parallels the large r_{C-H} value of the transition state. The α -alkylation makes the kinetics of R + HBr reaction high⁵ and its transition state early.

Enthalpies of formation

The *ab initio* calculated enthalpies of formation of various free radicals at 298 K are shown in Table 4. The error limits stated are practically similar to the accuracies of the determined heat

Table 4 Heat of formation values of the radicals determined from the $R + HX \rightleftharpoons RH + X$ ($X = \text{Br}$ or Cl) equilibrium

Radical	$\Delta_f H_{298}^\circ / \text{kJ mol}^{-1}$ calculated	$\Delta_f H_{298}^\circ / \text{kJ mol}^{-1}$ experim.	Ref. experim.
CH_3	149.3 ± 0.4	148.0 ± 3.7	25
CH_2Br	172.5 ± 1.3	145.2 ± 2.5	26
CH_2Cl	121.7 ± 2.1	173.0 ± 2.8	25
CHBr_2	180.0 ± 5	117.3 ± 3.1	27
CHBrCl	145.0 ± 8	188.3 ± 9	3
CHCl_2	92.2 ± 1.3	n.a. ^a	
CBr_3	195.3 ± 5	89.0 ± 3.0	27
CBr_2Cl	163.0 ± 8	207.5 ± 7	4
CBrCl_2	123.9 ± 8	n.a.	
CCl_3	70.6 ± 1.3	n.a.	
CH_3CH_2	120.4 ± 0.3	71.1 ± 2.5	28
CH_3CHCl	81.1 ± 0.5	120.7 ± 2.1	29
CH_2CICH_2	99.7 ± 0.5	76.5 ± 1.6	27
CH_3CCl_2	46.0 ± 0.8	93.0 ± 2.4	29
CHCl_2CH_2	90.1 ± 0.8	42.5 ± 1.7	27
<i>n</i> - C_3H_7	102.5 ± 0.4	n.a.	
iso- C_3H_7	83.6 ± 0.4	100.8 ± 2.1	5
2-iso- $\text{C}_3\text{H}_6\text{Cl}$	29.9 ± 0.6	86.0 ± 2.2	5
<i>n</i> - C_4H_9	80.7 ± 0.4	n.a.	
		80.9 ± 2.2	5

^a Not available.

of formation values of analogous molecules. The *ab initio* calculations were taken to be accurate; however, the calculated activation energies differ, generally between 1 and 4 kJ mol^{-1} , from the experimentally determined values. As a result, additional error limits of $\pm 2.4 \text{ kJ mol}^{-1}$ for the calculated enthalpies of formation are taken from the mean value of differences between the calculated and the experimental $\Delta_f H_{298}^\circ$ values in Table 4 (CHBr_2 and CBr_3 were ignored).

Summary

The enthalpies of formation of alkyl and halogenated alkyl radicals at 298 K were determined by *ab initio* calculations. The experimentally determined $R + \text{HBr}$ activation energies were combined with quantum chemically calculated $\text{Br} + \text{RH}$ activation energies to be used in a second-law method. Furthermore, the transition states of the equilibrium reactions were localized using *ab initio* calculations. The chemical nature of the transition state is described by an attractive energy release, which is inversely related to the free energy of activation of the reaction.

Acknowledgements

This research was supported by the University of Helsinki and the Center for Scientific Computing at Espoo (Finland).

References

- 1 J. A. Seetula, J. J. Russell and D. Gutman, *J. Am. Chem. Soc.*, 1990, **112**, 1347.
- 2 J. A. Seetula and D. Gutman, *J. Phys. Chem.*, 1991, **95**, 3626.
- 3 E. Tschuikow-Roux and S. Paddison, *Int. J. Chem. Kinet.*, 1987, **19**, 15.
- 4 K. D. King, D. M. Golden and S. W. Benson, *J. Phys. Chem.*, 1971, **75**, 987.
- 5 J. A. Seetula and I. R. Slagle, *J. Chem. Soc., Faraday Trans.*, 1997, **93**, 1709.
- 6 M. J. Frisch, G. W. Trucks, H. B. Schlegel, P. M. W. Gill, B. G. Johnson, M. A. Robb, J. R. Cheeseman, T. Keith, G. A. Petersson, J. A. Montgomery, K. Raghavachari, M. A. Al-Laham, V. G. Zakrzewski, J. V. Ortiz, J. B. Foresman, J. Cioslowski, B. B. Stefanov, A. Nanayakkara, M. Challacombe, C. Y. Peng, P. Y. Ayala, W. Chen, M. W. Wong, J. L. Andres, E. S. Replogle, R. Gomperts, R. L. Martin, D. J. Fox, J. S. Binkley, D. J. Defrees, J. Baker, J. P. Stewart, M. Head-Gordon, C. Gonzalez and J. A. Pople, GAUSSIAN 94, Revision B.1, Gaussian, Pittsburgh, PA, 1995.
- 7 J. B. Foresman and Æleen Frisch, *Exploring Chemistry with Electronic Structure Methods*, 2nd edn., Gaussian, Inc., Pittsburgh, 1996.
- 8 K. J. Laidler, *J. Chem. Educ.*, 1988, **65**, 540.
- 9 K. J. Laidler, *Pure Appl. Chem.*, 1996, **68**, 149.
- 10 M. W. Chase, Jr, C. A. Davies, J. R. Downey, Jr, D. J. Frurip, R. A. McDonald and A. N. Syverud, *J. Phys. Chem. Ref. Data*, 1985, **14**, supplement no 1.
- 11 J. Bickerton, M. E. M. da Piedade and G. Pilcher, *J. Chem. Thermodynam.*, 1984, **16**, 661.
- 12 S. A. Kudchadker and A. P. Kudchadker, *J. Phys. Chem. Ref. Data*, 1978, **7**, 1285.
- 13 D. A. Pittam and G. Pilcher, *J. Chem. Soc., Faraday Trans. 1*, 1972, **68**, 2224.
- 14 S. G. Lias, J. E. Bartmess, J. F. Lieleman, J. L. Holmes, R. D. Lerein and W. G. Mallard, *J. Phys. Chem. Ref. Data*, 1988, **17**, supplement no 1.
- 15 J. Chao, A. S. Rodgers, R. C. Wilhoit and B. J. Zwolinski, *J. Phys. Chem. Ref. Data*, 1974, **3**, 141.
- 16 J. A. Seetula, *J. Chem. Soc., Faraday Trans.*, 1998, **94**, 3561.
- 17 J. M. Nicovich, C. A. van Dijk, K. D. Kreutter and P. H. Wine, *J. Phys. Chem.*, 1991, **95**, 9890.
- 18 Y. Chen, A. Rauk and E. Tschuikow-Roux, *J. Phys. Chem.*, 1991, **95**, 9900.
- 19 J. J. Russell, J. A. Seetula, R. S. Timonen, D. Gutman and D. F. Nava, *J. Am. Chem. Soc.*, 1988, **110**, 3084.
- 20 M. A. Nazar, J. C. Polanyi and W. J. Skrlac, *Chem. Phys. Lett.*, 1974, **29**, 473.
- 21 J. I. Steinfeld, J. S. Francisco and W. L. Hase, *Chemical Kinetics and Dynamics*, 2nd edn., Prentice-Hall, New Jersey, 1999.
- 22 G. S. Hammond, *J. Am. Chem. Soc.*, 1955, **77**, 334.
- 23 M. H. Mok and J. C. Polanyi, *J. Chem. Phys.*, 1969, **51**, 1451.
- 24 D. Krajnovich, Z. Zhang, F. Huisken, Y. R. Shen and Y. T. Lee, *Phys. Electron. At. Collisions*, Invited Pap. Int. Conf., 12th, 1981, p. 733.
- 25 J. A. Seetula and I. R. Slagle, *13th Int. Symp. on Gas Kinetics*, University College Dublin, Dublin, Ireland, 1994, p. 148.
- 26 J. J. Russell, J. A. Seetula, S. M. Senkan and D. Gutman, *Int. J. Chem. Kinet.*, 1988, **20**, 759.
- 27 J. A. Seetula, *J. Chem. Soc., Faraday Trans.*, 1996, **92**, 3069.
- 28 J. W. Hudgens, R. D. Johnson III, R. S. Timonen, J. A. Seetula and D. Gutman, *J. Phys. Chem.*, 1991, **95**, 4400.
- 29 J. A. Seetula, *J. Chem. Soc., Faraday Trans.*, 1998, **94**, 891.
- 30 L. Pauling, *Nature of the Chemical Bond*, 3rd edn., Cornell University Press, Ithaca, NY, 1960.
- 31 J. H. Sullivan and N. Davidson, *J. Chem. Phys.*, 1951, **19**, 143.